A practical method to avoid zero-point leak in molecular dynamics calculations: Application to the water dimer

Gábor Czakó,[a] Alexey L. Kaledin, and Joel M. Bowman[b]
Department of Chemistry and Cherry L. Emerson Center for Scientific Computation, Emory University, Atlanta, Georgia 30322, USA

(Received 1 March 2010; accepted 8 April 2010; published online 22 April 2010)

We report the implementation of a previously suggested method to constrain a molecular system to have mode-specific vibrational energy greater than or equal to the zero-point energy in quasiclassical trajectory calculations [J. M. Bowman *et al.*, J. Chem. Phys. **91**, 2859 (1989); W. H. Miller *et al.*, J. Chem. Phys. **91**, 2863 (1989)]. The implementation is made practical by using a technique described recently [G. Czakó and J. M. Bowman, J. Chem. Phys. **131**, 244302 (2009)], where a normal-mode analysis is performed during the course of a trajectory and which gives only real-valued frequencies. The method is applied to the water dimer, where its effectiveness is shown by computing mode energies as a function of integration time. Radial distribution functions are also calculated using constrained quasiclassical and standard classical molecular dynamics at low temperature and at 300 K and compared to rigorous quantum path integral calculations. © *2010 American Institute of Physics*. [doi:10.1063/1.3417999]

I. INTRODUCTION

The quasiclassical trajectory (QCT) method is widely used in gas-phase reaction dynamics calculations. In this method molecular vibrations are typically initially "quantized," most commonly by giving reactant molecules vibrational energy equal to the quantum mechanical zero-point energy (ZPE) and if desired rovibrationally excited states.[1] This initial condition has been shown over many years to produce results for chemical reactions that are far more accurate and realistic when compared to accurate quantum calculations than if no vibrational energy is initially given to molecules. The method was originally introduced for atom-diatom reactions[1] and then used very widely for this class of reactions. It has also been used recently for polyatomic reactants;[2–7] however, in this context the application is problematic because of what is now generally known as "zero-point leak" (ZPL).[8–11] This leak is largely due to the use of an approximate harmonic model for vibrational quantization instead of "exact" semiclassical quantization of multimode systems which remains a very challenging computational problem, even for the ZPE. (Note that ZPL may result from classical chaotic motion as discussed in Ref. 12.) In any approximate model classical intramolecular vibrational relaxation of the ZPE from high-frequency modes to lower frequency ones will occur. The rate at which it occurs is of course the practical issue. In reactive scattering it often occurs on a time scale long compared to the reaction time.[7] In this case it appears that ZPL is not a major concern. (It is worth noting that these issues are not present for diatomic reactants, i.e., for A+BC reactions.)

As the system size grows so does the total ZPE and with it the concern about ZPL. For physical/chemical processes in the condensed phase ZPL is clearly a concern and in fact ZPE is generally ignored in classical molecular dynamics (MD) simulations in the condensed phase. Instead canonical or microcanonical sampling of the classical phase space is done. Roughly speaking in the former case this amounts to giving each vibrational mode *RT* of total energy, which at room temperature is roughly 0.6 kcal/mol. However the ZPE of a typical OH stretch is roughly eight times larger. An obvious consequence of this additional energy for a realistic Morse-like OH stretch potential is an increase in the average bond length and a broader radial distribution function (RDF) compared to the results using room temperature classical internal energy. Indeed, recent approximate/semiquantum approaches to the study of various properties of water have clearly shown the importance of ZPE,[11–17] and now point to the absence of this as a significant issue in standard classical MD simulations. (It is also worth noting that Habershon and Manolopoulos[11] recently pointed out the ZPL issue in some of these semiquantum approaches.)

So, motivated both by the importance of ZPE for simulations involving water (and more generally for systems with hydride modes) and the issue of ZPL we have reinvestigated an active approach introduced in 1989 (Refs. 8 and 9) to prevent ZPL. (Other approaches to deal with ZPL have been proposed and these have recently been reviewed in Ref. 11 and so for brevity, we refer the interested reader to that paper.) In this approach a hard shell representing the ZPE in a given mode is introduced in the phase space of each pair of canonically conjugate coordinate and momentum. If a trajectory attempts to cross this shell it is "kicked away" by flipping the sign of the momentum. We will also refer to this method as "constrained dynamics."

In order to generalize this method to realistic general systems, Miller *et al.*[9] suggested using the instantaneous normal-mode method at each time step. Apart from the early

[a]Electronic mail: czako@chem.elte.hu.
[b]Electronic mail: jmbowma@emory.edu.

applications for Al_3 and C_2H_6 (see Ref. 10), this suggestion has not been implemented for other systems to our knowledge, perhaps in part because of the associated well-known issues with imaginary frequencies and also because the full normal-mode analysis at every time step renders the method very computationally intensive for large systems.

Here we propose a different approach to implement the constrained "kick" dynamics to prevent ZPL. The approach is based on a recent publication[7] where the goal was to assign harmonic quantum numbers to the polyatomic products of the $F+CHD_3$ reaction, CD_3 and CHD_2. The method is to transform Cartesian coordinates and momenta of these polyatomics to the normal coordinates of a minimum that is determined by a steepest descent path from the instantaneous configuration of the molecular system. We note that Stillinger and Weber[18] also used a steepest descent method to assign any arbitrary configuration in liquids and solids to a minimum. (A related normal-mode approach has also been suggested recently by Espinosa-García,[4,19] and indeed much earlier by Schatz,[20] who used a more rigorous semiclassical analysis of product vibrational motion.) Then by simply relating the instantaneous configuration and momenta to the normal-mode coordinates and momenta the analysis of mode energies was done. This approach has the advantage that only real-frequency modes are used in the analysis, and second for many (perhaps all) time steps the same minimum and therefore the same normal modes can be used in the analysis. Clearly this method can immediately be used to apply the hard-shell constraint to prevent ZPL. We do that here by applying these combined methods to the water dimer. This application is motivated in large part by the above discussion about the importance of the effects of ZPE in simulations of water.

This paper is organized as follows. In Sec II we briefly review the method and its implementation for $(H_2O)_2$ and we show how to apply the active constraint introduced in Refs. 8 and 9. The computational details of the different dynamics investigated in the present study are given in Sec. III. We present the mode energies and OO-distance of $(H_2O)_2$ as a function of time and RDFs obtained from different dynamics simulations in Sec. IV. The paper is ended by conclusions and remarks (Sec. V) on possible techniques, which can be further investigated in the future to make the method more efficient for larger systems.

II. METHOD

First, standard normal-mode initial conditions[2] are applied for each trajectory. Harmonic ZPE is given to each mode, standard transformations to Cartesian coordinates and momenta are made, and small adjustments to the total angular momentum are applied such that it equals zero. Each trajectory is propagated and at nearly every time step a "reverse-normal-mode analysis" is done, as described in detail in Ref. 7. Here we give the details of the present implementation for the water dimer.

Let the Cartesian coordinates and corresponding velocities in the center of mass frame be denoted by $\mathbf{r}_i$ and $\mathbf{v}_i$ ($i=1,2,\ldots,N$), respectively. ($N=6$ for the present application.) Since the molecule configuration is generally not at a stationary point, we need to relate the actual configuration to normal-mode displacements of a reference minimum geometry. The potential energy surface (PES) of $(H_2O)_2$ has eight equivalent minima denoted as $\mathbf{r}_i^{\mathrm{eq}}(i_{\min})$, where $i_{\min}=1,2,\ldots,8$. In the present implementation for $(H_2O)_2$ we determine the reference geometry by minimizing the expression

$$\sum_{i=1}^{N} \|\mathbf{r}_i - \mathbf{C}(\theta,\phi,\psi)\mathbf{r}_i^{\mathrm{eq}}(i_{\min})\| \tag{1}$$

with respect to the three Euler angles (θ,ϕ,ψ) and $i_{\min}$. In Eq. (1) $\mathbf{C}$ is an orthogonal rotational matrix depending on the Euler angles. The determined reference structure (denoted as $\mathbf{r}_i^{\mathrm{eq}}$) is one of the minima on the PES with an optimized orientation (in the present calculations this is always the starting global minimum for the *constrained* trajectories); thus, a normal-mode analysis there provides nonzero *real* frequencies ω_k ($k=1,2,\ldots,3N-6$) and the orthogonal transformation matrix $\mathbf{l}$. Normal coordinates, Q_k ($k=1,2,\ldots,3N-6$), and conjugate momenta, P_k ($k=1,2,\ldots,3N-6$), can then be obtained using the straightforward transformation from Cartesian displacement coordinates ($\Delta\mathbf{r}_i=\mathbf{r}_i-\mathbf{r}_i^{\mathrm{eq}}$) and $\mathbf{v}_i$, respectively. Note that this approach should not be confused with the *instantaneous* normal-mode method in which a normal-mode analysis is done at the given configuration, which, in general, leads to *imaginary* frequencies and potentially large mode coupling, which is ignored if one restricts attention to only the real-frequency modes.

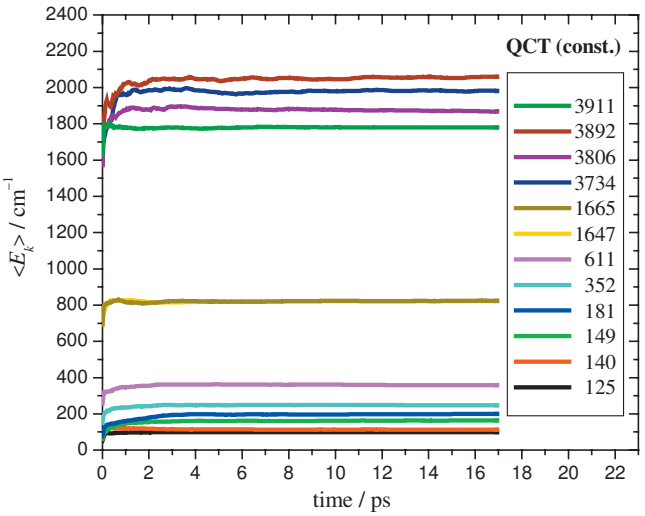

FIG. 1. Expectation values of the harmonic vibrational energies corresponding to the normal modes of $(H_2O)_2$ as a function of integration time obtained from constrained QCT (0 K) calculations. The harmonic energies are averaged over 100 trajectories and the time interval $[0,t]$. The initial quasiclassical ground vibrational state of $(H_2O)_2$ was set by standard normal-mode sampling. The harmonic frequencies corresponding to the 12 normal modes are given in cm^{-1}.

Employing these normal coordinates and momenta the vibrational energy for each normal mode can be calculated as

$$E_k = \frac{P_k^2}{2} + \frac{\omega_k^2 Q_k^2}{2}, \quad k = 1,2,\ldots,3N-6, \tag{2}$$

and a noninteger classical harmonic action number for each mode can be obtained (in atomic units) as

$$n_k = \frac{E_k}{\omega_k} - \frac{1}{2}, \quad k = 1,2,\ldots,3N-6. \tag{3}$$

Having determined the actual harmonic action numbers at a given integration step [*step* in Eq. (5)], we apply the active constraint employing the following equations:

$$P_k = \sum_{i=1}^{N} \sqrt{m_i}\mathbf{l}_{ki}\mathbf{v}_i, \quad k = 1,2,\ldots,3N, \tag{4}$$

$$P_k^{\text{new}} = -P_k \begin{cases} \text{if } n_k < n_{\min} & \text{and} \quad n_k(step) < n_k(step-1) \\ \text{if } n_k > n_{\max} & \text{and} \quad n_k(step) > n_k(step-1) \end{cases} \quad k = 1,2,\ldots,3N-6, \tag{5}$$

$$\mathbf{v}_i^{\text{new}} = \sum_{k=1}^{3N} \mathbf{l}_{ki} P_k^{\text{new}}/\sqrt{m_i} \quad \text{and} \quad \mathbf{r}_i^{\text{new}} = \mathbf{r}_i. \tag{6}$$

At this point a few comments are in order.

(1) In Eq. (4) all the $3N$ momenta are computed.
(2) According to Refs. 8 and 9 if n_k is less than zero the sign of P_k is changed. In practice [see Eq. (5)] we have applied a window constraint such that the momentum is flipped only if n_k is not in the interval $[n_{\min}, n_{\max}]$.
(3) In Eq. (5) we also consider if n_k has decreased or increased since the previous integration step (*step*–1), i.e., n_k goes to the right or wrong direction.
(4) The momentum flip conserves the mode energy since it depends on the square of P_k [see Eq. (2)].
(5) Eq. (6) conserves the total energy exactly since $\mathbf{l}$ is an orthogonal matrix and comment (1) ensures the lack of any numerical errors due to the uncertainties of the 6 "zero" frequencies and corresponding momenta.
(6) We continue to propagate the trajectory in the Cartesian space using the new velocities ($\mathbf{v}_i^{\text{new}}$). The constraint has no effect on the Cartesian coordinates.

For future use we refer to unconstrained trajectories as being those with the usual quasiclassical conditions but without preserving the ZPE. These are the standard QCT results. In addition we will also consider standard MD calculations in which ZPE is not initially added to each mode but a purely classical phase space sampling is used instead, as described below in Sec. III.

III. COMPUTATIONAL DETAILS

We have computed 100 constrained and 100 unconstrained QCTs for $(H_2O)_2$ using a recent *ab initio*-based full-dimensional PES called HBB2 (Ref. 21). All trajectories were initiated from the global minimum and coordinates and momenta were sampled randomly from the normal modes, in the usual way,[2] with harmonic ZPE given to each normal mode. The energy interval noted above corresponds to an action number interval of ± 0.1 for each mode. So provided the energy of the given mode is within this interval no momentum switching in that mode was done.

Trajectories were integrated using the velocity Verlet algorithm.[22] For both unconstrained and constrained trajectories the total integration time was roughly 17 ps. For the latter the normal-mode/energy analysis was performed at every fifth time step. A time step of 0.242 fs was used for unconstrained trajectories and a smaller time step, 0.0484 fs, was used for the constrained trajectories. (Evidently the momentum flipping, which is equivalent to an impulse, requires a smaller time step to achieve good energy conservation.)

These constrained and unconstrained trajectories with these initial conditions obviously correspond to 0 K. We will also consider constrained and standard MD trajectories run at 300 K. The initial conditions for the constrained QCTs at temperature T are identical to those at 0 K but with the initial mode energies (in atomic units) given by $\omega_k[1/2 + 1/(\exp(\omega_k/RT)-1)]$ based on the quantum mechanical mean energy of a harmonic oscillator. The interval for applying the momentum flip is $[-0.1,\ 0.1+a/(\exp(\omega_k/RT)-1)]$ for each harmonic action number as this achieves the goal of preventing significant ZPL and the dissociation of the dimer. The real parameter a was set to 1 in this study. Standard MD trajectories were run for 24.5 ps after selecting roughly 100 initial phase points $(\mathbf{p},\mathbf{q})$ at 10 and 300 K by sampling $\mathbf{p}$ from the normal distribution $\exp(-\mathbf{p}^2/(2mRT))$ and $\mathbf{q}$ from $\exp(-V(\mathbf{q})/RT)$ by performing a random walk at each temperature in 18 dimensions.[23] For more details about the classical MD, see Ref. 21.

The quantum mechanical thermal energy contributions at 300 K above $\omega_k/2$ (the frequencies are given in Fig. 1) are 152, 146, 143, 131, 80, and 34 cm^{-1} for the intermolecular modes in order of increasing frequency and <1 cm^{-1} for all the intramolecular modes of $(H_2O)_2$, whereas the classical RT corresponds to 208 cm^{-1} for each mode. Thus, the total energy is about 10 100 and 10 800 cm^{-1} in the QCT simulations at 0 and 300 K, respectively. In the standard classical MD calculations the total energy is lesser, i.e., 150 and 1900 cm^{-1} on average at 10 and 300 K, respectively.

The path integral[24] Monte Carlo (PIMC) simulations

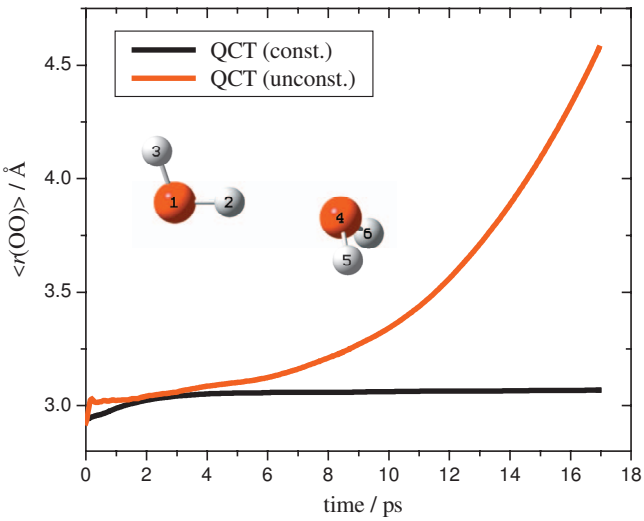

FIG. 2. Expectation values of the OO-distance of $(H_2O)_2$ as a function of integration time obtained from constrained and unconstrained QCT (0 K) calculations initialized in the ground vibrational state of $(H_2O)_2$ using standard normal-mode sampling. The $r(OO)$ is averaged over 100 trajectories and the time interval $[0,t]$.

provide our benchmark quantum mechanical RDFs at 6.25 and 300 K. The temperature of 6.25 K is low enough to ensure that all the modes of the dimer remain in their zero-point level and so provide the 0 K benchmark results. Numerical evaluation of the density operator $\exp(-\beta\hat{H}) = [\exp(-(\beta/P)\hat{H})]^P$ requires that the effective inverse temperature β/P is sufficiently small.[25] A suitable criterion is to take P large enough so that the product $(\beta/P)\omega$ is smaller than 1, where ω is the highest fundamental frequency of the system. Following some exploratory calculations, we chose $P=2^{12}$ (4096), which makes the target product with the OH fundamental $\sim$0.2 at 6.25 K. For 300 K simulations, we used $P=2^7$ (128) to yield the target product $\sim$0.14. The Monte Carlo procedure was carried out using the standard Metropolis sampling methods[23] developed for PIMC simulations. In this work we utilized the staging algorithm to sample paths.[26] The number of neighboring "beads" to be sampled simultaneously in the staging procedure was adjusted to keep the acceptance ratio around 40%; the final chosen value for the staging parameter was 12 (17), which resulted in the overall acceptance ratio of 38% (42%), at 6.25 (300) K. In all, we averaged the RDFs from eight independent PIMC calculations with each run extending to 50 000 (100 000) imaginary time steps for 6.25 (300) K. The resulting statistics showed tightly converged RDFs (to within about 1% standard deviation) for all atom pairs: OO, OH, and HH.

IV. RESULTS AND DISCUSSIONS

Figure 1 shows the time evolution of the 12 harmonic mode energies of $(H_2O)_2$ for constrained dynamics. As seen the constrained QCT (0 K) method described above is successful in keeping the mode energies very close to the ZPE. By contrast if no constraint is employed, some normal-mode quantum numbers increase very rapidly in the first 0.1 ps. Since the energy flows from the intramolecular modes to the intermolecular modes, the water dimer exhibits extremely large amplitude motion and therefore, the normal-mode analysis, which is based on small displacements from a minimum energy structure, breaks down. The fastest quantum number increase at $t>6$ ps can be observed in the cases of the two modes (149 and 181 cm^{-1}) that have O–O stretching character. It is interesting to see that there is one intermolecular mode (611 cm^{-1}) that remains close to the zero-point level (without any constraint) during the 17 ps integration time.

The (highly accurate) electronic dissociation energy (D_e) of water dimer on the HBB2 PES is 1740 cm^{-1},[21] which is lesser than the total energy in the QCT simulations and so dissociation of the dimer can certainly occur for unconstrained trajectories. Thus we monitored the OO-distance as function of time for constrained and unconstrained trajectories. Figure 2 shows the expectation value (obtained from 100 trajectories) of the OO-distance of $(H_2O)_2$ as a function of time. The constrained QCT provides an almost steady $\langle r(OO)\rangle$, whereas $\langle r(OO)\rangle$ begins to increase rapidly at around 4 ps if no constraint is employed. At $t=17$ ps the unconstrained $\langle r(OO)\rangle$ is about 4.5 Å (with a large variance) instead of around 3.0 Å; thus, the utility of the constraint is clearly shown for this observable.

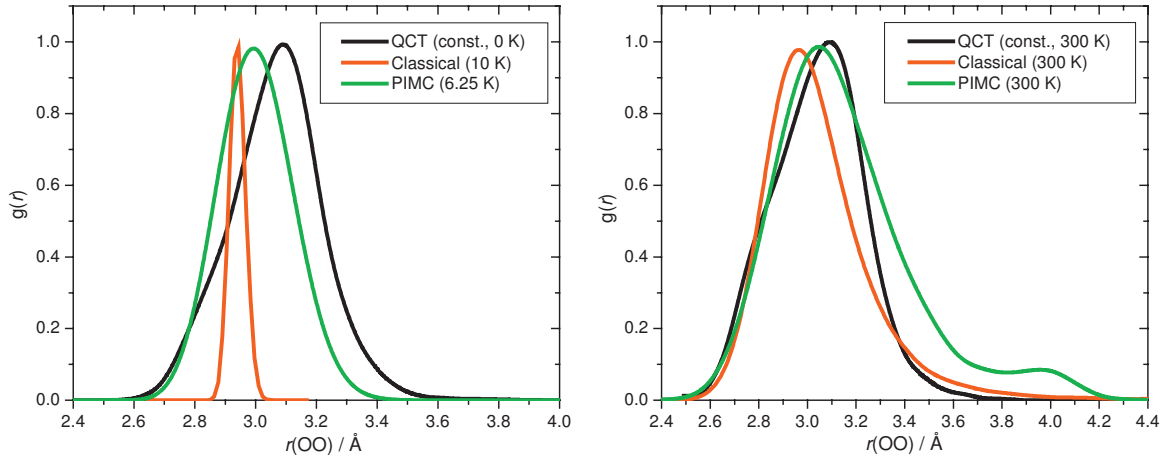

FIG. 3. O–O RDFs of $(H_2O)_2$ obtained from different MD simulations. Each RDF is normalized having a maximum value of 1.

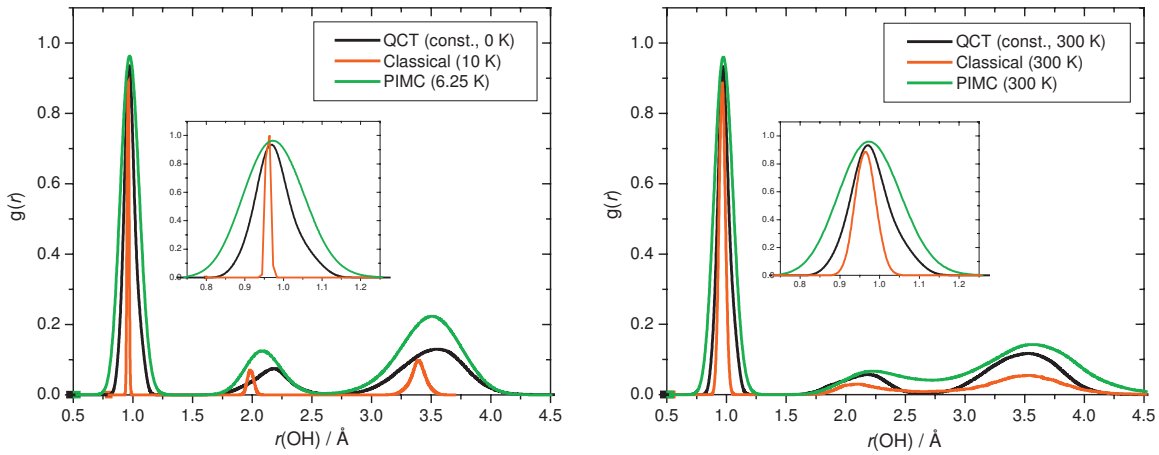

FIG. 4. O–H RDFs of $(H_2O)_2$ obtained from different MD simulations. Each RDF is normalized having a maximum value of 1.

We have computed the RDFs of $(H_2O)_2$ using (a) constrained QCT at 0 and 300 K, (b) classical MD at 10 and 300 K, and (c) PIMC at 6.25 and 300 K calculations. Figures 3–5 show the O–O, O–H, and H–H RDFs of $(H_2O)_2$, respectively. The classical MD at 10 K gives too narrow RDFs even if the long-range intermolecular distances are considered. This is expected because the classical MD neglects the ZPE of the system and 10 K corresponds to very low energy. If we increase the temperature to 300 K in a classical simulation, the RDFs of the *intermolecular* distances become slightly wider than the PIMC (6.25 K); however, these classical (300 K) RDFs are still significantly narrower than those from PIMC (300 K). Therefore, we can say that 300 K thermal energy roughly corresponds to the quantum ZPE of the intermolecular modes. On the other hand in the case of the *intramolecular* OH and HH RDFs the quantum PIMC (in agreement with the QCT) results show that the thermal effect is negligible since the PIMC (QCT) intramolecular RDFs are roughly the same at 6.25 (0) and 300 K. Considering the classical results a huge temperature effect can be seen; the 300 K RDFs are much wider than the 10 K ones. However, the classical intramolecular results at 300 K are still much more localized than the benchmark PIMC (6.25 and 300 K) RDFs. The constrained QCT intramolecular RDFs are in much better agreement with PIMC than the classical MD ones, even if a temperature of 300 K is employed classically.

V. CONCLUSIONS AND FINAL REMARKS

The comparisons shown here between the constrained quasiclassical and benchmark RDFs directly confirm the importance of ZPE for these properties. As noted in Sec. I the importance of ZPE has already been well established for a variety of properties of bulk water and we show this here for the water dimer. Of course it remains to be seen whether the current approach of constraining ZPE can be used for bulk water. There will clearly be an increase in computational effort mainly, in doing the analysis of mode energies. If the system relaxes to a known minimum at each analysis step then the normal-mode eigenvalues and eigenvectors can be reused for this analysis and no further normal-mode analysis is needed. Furthermore, our current test computations show that the application of the constraint is not necessary at every 0.242 fs. Other possibilities that we are currently investigating include applying the constraint only to high-frequency modes, i.e., the monomer stretches and bands. This should simplify the analysis and perhaps lead to less frequent momentum flipping than was done here.

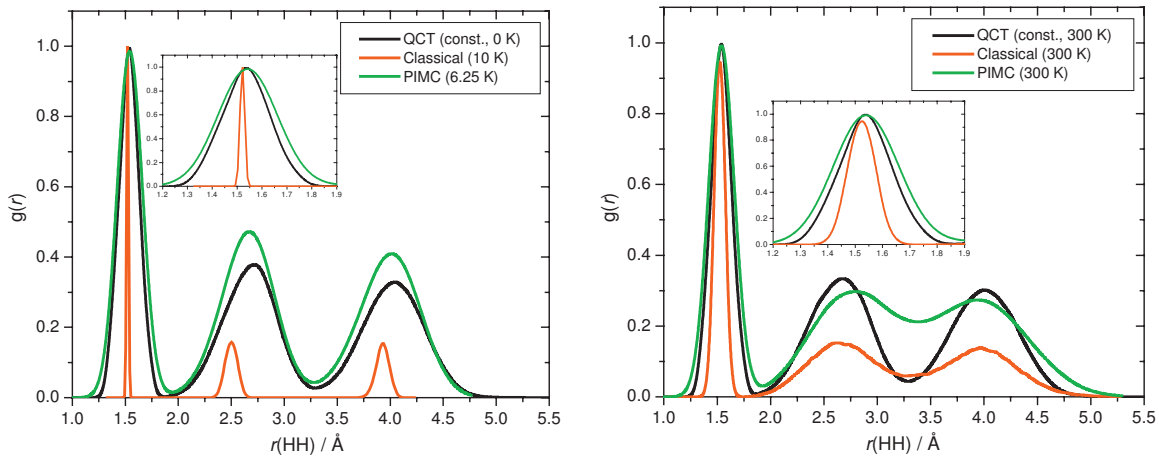

FIG. 5. H–H RDFs of $(H_2O)_2$ obtained from different MD simulations. Each RDF is normalized having a maximum value of 1.

The application of this approach to a variety of properties seems straightforward. For example, the self-diffusion constant should be readily obtainable using constrained trajectories. Calculation of spectra, however, is more problematic. The reason for this is using the standard Fourier transform relationship between a correlation function and spectrum will have to cope with a "noisy" background on what should be a standard oscillatory correlation function. We plan to investigate this in detail in the future.

It should also be noted that the method to prevent ZPE leak described here has its limitations. It is not clear that it can be used to describe chemical reactions where bonds break. In this case assigning a minimum configuration that can be used for the normal-mode analysis as the system passes near a saddle point appears to be problematic. However, the method can be useful for preventing intramolecular vibrational relaxation in bimolecular reactions prior to the collision.

Finally, we note that the "on the fly" normal-mode analysis applied here for computing mode energies at each time step could be a useful tool for any (quasi-) classical MD analyses if one wishes to track the energy flow between the normal modes of a molecular system.

ACKNOWLEDGMENTS

Financial support from the National Science Foundation (Grant No. CHE-0848233) is gratefully acknowledged.

[1] M. Karplus, R. N. Porter, and R. D. Sharma, J. Chem. Phys. **40**, 2033 (1964).
[2] W. L. Hase, *Encyclopedia of Computational Chemistry* (Wiley, New York, 1998), pp. 399–407.
[3] J. F. Castillo, F. J. Aoiz, and L. Bañares, J. Chem. Phys. **125**, 124316 (2006).
[4] J. Espinosa-García, J. L. Bravo, and C. Rangel, J. Phys. Chem. A **111**, 2761 (2007).
[5] J. P. Layfield, A. F. Sweeney, and D. Troya, J. Phys. Chem. A **113**, 4294 (2009).
[6] G. Czakó, B. C. Shepler, B. J. Braams, and J. M. Bowman, J. Chem. Phys. **130**, 084301 (2009).
[7] G. Czakó and J. M. Bowman, J. Am. Chem. Soc. **131**, 17534 (2009); J. Chem. Phys. **131**, 244302 (2009).
[8] J. M. Bowman, B. Gazdy, and Q. Sun, J. Chem. Phys. **91**, 2859 (1989).
[9] W. H. Miller, W. L. Hase, and C. L. Darling, J. Chem. Phys. **91**, 2863 (1989).
[10] G. H. Peslherbe and W. L. Hase, J. Chem. Phys. **100**, 1179 (1994).
[11] S. Habershon and D. E. Manolopoulos, J. Chem. Phys. **131**, 244518 (2009).
[12] D.-h. Lu and W. L. Hase, J. Chem. Phys. **89**, 6723 (1988).
[13] S. Habershon, T. E. Markland, and D. E. Manolopoulos, J. Chem. Phys. **131**, 024501 (2009).
[14] F. Paesani and G. A. Voth, J. Phys. Chem. B **113**, 5702 (2009).
[15] J. A. Poulsen, G. Nyman, and P. J. Rossky, Proc. Natl. Acad. Sci. U.S.A. **102**, 6709 (2005).
[16] T. F. Miller III and D. E. Manolopoulos, J. Chem. Phys. **123**, 154504 (2005).
[17] J. Liu, W. H. Miller, F. Paesani, W. Zhang, and D. A. Case, J. Chem. Phys. **131**, 164509 (2009).
[18] F. H. Stillinger and T. A. Weber, Science **225**, 983 (1984).
[19] J. C. Corchado and J. Espinosa-García, Phys. Chem. Chem. Phys. **11**, 10157 (2009).
[20] G. C. Schatz, in *Molecular Collision Dynamics*, edited by J. M. Bowman (Springer-Verlag, Berlin, 1983), pp. 25–60.
[21] A. Shank, Y. Wang, A. Kaledin, B. J. Braams, and J. M. Bowman, J. Chem. Phys. **130**, 144314 (2009).
[22] L. Verlet, Phys. Rev. **159**, 98 (1967).
[23] N. Metropolis, A. W. Rosenbluth, M. N. Rosenbluth, A. H. Teller, and E. Teller, J. Chem. Phys. **21**, 1087 (1953).
[24] R. P. Feynman and A. R. Hibbs, *Quantum Mechanics and Path Integrals* (McGraw-Hill, New York, 1965).
[25] D. M. Ceperley, Rev. Mod. Phys. **67**, 279 (1995).
[26] W. Janke and T. Sauer, J. Chem. Phys. **107**, 5821 (1997).